ARTICLES

Oligosilane Chain-Length Dependence of Electron Transfer of Zinc Porphyrin−Oligosilane−Fullerene Molecules

Mikio Sasaki,[†] Yuki Shibano,[‡] Hayato Tsuji,*[,‡,§] Yasuyuki Araki,[†] Kohei Tamao,*[,‡,||] and Osamu Ito*[,†]

Institute of Multidisciplinary Research for Advanced Materials, Tohoku University, Katahira, Aoba-ku, Sendai 980-8577, Japan, and International Research Center for Elements Science (IRCELS), Institute for Chemical Research, Kyoto University, Uji, Kyoto 611-0011, Japan

Received: October 13, 2006; In Final Form: February 15, 2007

A new series of zinc porphyrin−fullerenes bridged by flexible oligosilane chains $ZnP-[Si_n]-C_{60}$ ($n = 1-5$) was synthesized, and the photophysical properties of these molecules were investigated using steady-state and time-resolved spectroscopic methods. The spectral observations can be well explained by assuming the coexistence of extended conformers and folded conformers, that is, the observed emissions are from the extended conformers while the folded conformers form very short lifetime nonfluorescent excited-state charge-transfer (CT) complexes. Time-resolved transient absorption spectra suggest the generation of intramolecular radical-ion pairs that have sub-microsecond lifetimes. With the number of silicon atoms of the bridged oligosilane, the lifetimes of the radical-ion pairs do not vary regularly, indicating that intramolecular collision of the radical-cation moiety with the radical-anion moiety controls the charge-recombination rate. The attenuation factor of the electron transfer of the silicon chain was evaluated by the bridge-length dependence of charge-separation rate to be 0.16 Å^{-1} on the basis of the oligosilane chain-length dependence of fluorescence lifetimes. This is the first evaluation of the attenuation factor for the one-dimensional Si−Si chain to the best of our knowledge.

1. Introduction

Photoinduced electron transfer (ET) processes in a covalently linked donor (D) and acceptor (A) with bridge (B) systems have been studied in recent decades to understand and mimic the well-arranged natural photosynthetic systems.[1] These studies have clarified the mechanisms of the ET, which strongly depends on the electron-donating and accepting abilities of both the D and the A moieties, as well as the electronic couplings between D−B and B−A. In strongly coupled systems, a hopping mechanism dominates the electron or hole transfer,[2] while a superexchange mechanism governs the carrier transfer in weakly coupled systems.[3]

The flexibility of the bridge also affects the photoexcited-state dynamics. In D−B−A systems in which a rigid bridge separates the D and A moieties from each other, the relationship between the ET rate and the bridge length can be described in terms of the through-bond couplings, such as the attenuation factors (β) of the bridges.[4] On the other hand, in D−B−A systems with flexible bridges, ET usually competes with exciplex formation,[5] and the efficiencies of these processes are
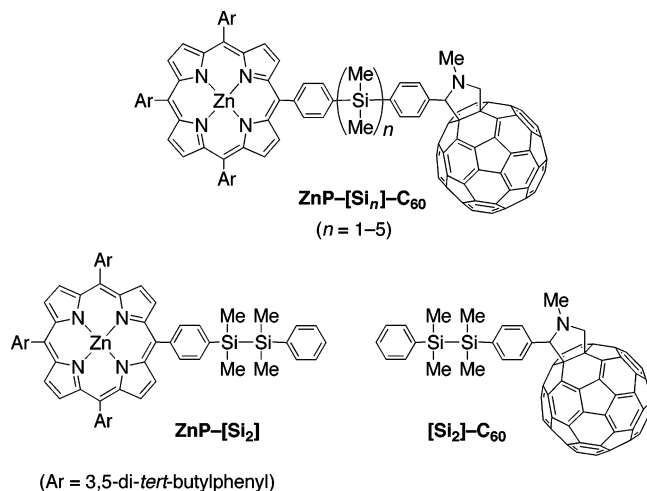
* To whom correspondence should be addressed. Phone, fax: +81-22-217-5608, E-mail: ito@tagen.tohoku.ac.jp.
† Tohoku University.
‡ Kyoto University.
§ Present address: Department of Chemistry, Graduate School of Science, The University of Tokyo, Bunkyo-ku, Tokyo 113-0033, Japan.
|| Present address: RIKEN Frontier Research System, Wako, Saitama 351-0198, Japan.

Figure 1. Molecular structures of $ZnP-[Si_n]-C_{60}$, $ZnP-[Si_2]$, and $[Si_2]-C_{60}$.
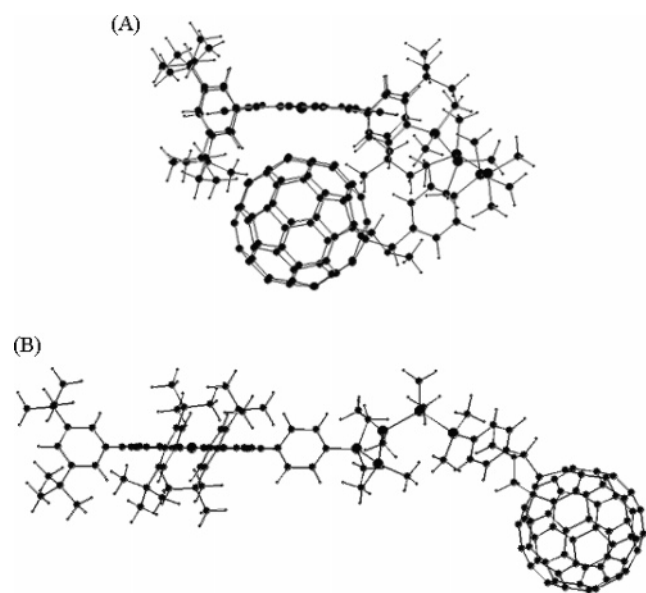

Figure 2. Representative structures of folded (A) and extended (B) conformers of $ZnP-[Si_5]-C_{60}$ optimized with molecular mechanics method using UFF force field.

affected by the relative geometry between D and A, as well as the properties of the media, such as the polarities and viscosities of solvents.

In photoinduced ET systems, porphyrins and fullerenes are widely used as D and A, respectively, because of their favorable features, such as electron-donating or accepting abilities, long lifetimes of triplet-excited (T_1) states, and wide absorptions in the visible region as good light-harvesting ensembles.[6] In most cases, various carbon-based bridges were used in the porphyrin—fullerene systems.[7]

In very recent studies, we reported the occurrence of photoinduced ET and the silicon chain-conformation dependence of the ET in zinc porphyrin (ZnP)—[60]fullerene (C_{60}) dyads linked with 1,2-dialkynyldisilane and with conformation-constrained tetrasilanes.[8] We chose silicon-catenated chains as bridges in the $ZnP-C_{60}$ because they are expected to construct other classes of carrier-transporting media than the preceding carbon-based bridges. Oligosilanes and polysilanes show σ-electron delocalization along the silicon framework (σ-conjugation),[9] which is responsible for their unique photophysical and electronic properties, such as ultraviolet light emission and hole-transfer ability. Although the carrier-hopping probabilities
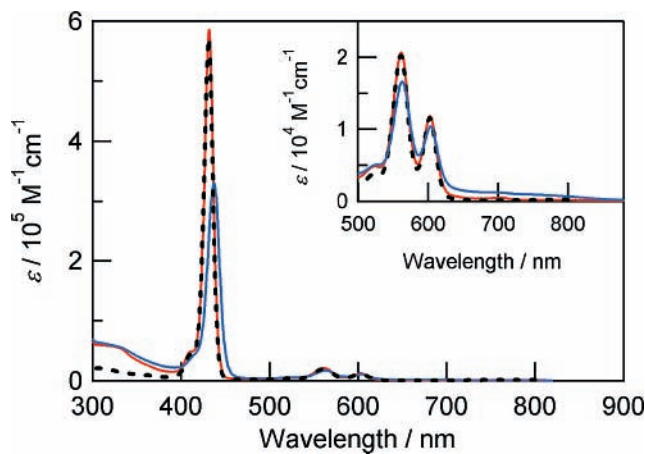

Figure 3. Steady-state absorption spectra of $ZnP-[Si_1]-C_{60}$ (red solid line), $ZnP-[Si_5]-C_{60}$ (blue solid line), and $ZnP-[Si_2]$ (black dashed line) in PhCN. Inset: Spectra of NIR region.

between molecules in thin polysilane films have been well investigated,[10] carrier-transport abilities along a discrete oligo-silane chain have not yet been experimentally evaluated to the best of our knowledge.

In the present article, we describe the synthesis of a new series of oligosilane-bridged $ZnP-C_{60}$ molecules, $ZnP-[Si_n]-C_{60}$ ($n = 1-5$, Figure 1), and the investigation of the bridge-length dependence of their photophysical properties, using steady-state and time-resolved spectroscopic methods.

2. Results

A series of zinc porphyrin—oligosilane—fullerene molecules $ZnP-[Si_n]-C_{60}$ and the reference compounds $ZnP-[Si_2]$ and $[Si_2]-C_{60}$ have been synthesized in the same manner as the previous report (see Scheme S1 in Supporting Information).[8b]

2.1. ^{1}H NMR. Because of the flexibility of the oligosilane bridge, the conformation of $ZnP-[Si_n]-C_{60}$ should be considered. First of all, the ^{1}H NMR spectra of $ZnP-[Si_n]-C_{60}$ suggest the existence of folded conformers (in Figure 2A an example of optimized folded conformer obtained by the molecular mechanics; $n = 5$), in which the ZnP and C_{60} moieties are spatially placed close to each other. For example, the signals of the β protons of the ZnP ring of $ZnP-[Si_n]-C_{60}$ are shifted upfield by $0.02-0.2$ ppm compared to those of the corresponding precursor $ZnP-[Si_n]-CHO$. This phenomenon can be explained by the shielding effect of the five-membered ring moiety of C_{60} or by the reduction in the ring current of the ZnP ring with the attachment of an electron-withdrawing C_{60}.[11,12] The signals of the three protons of the pyrrolidine moiety of $ZnP-[Si_2]-C_{60}$ (δ_H 3.54, 4.27, and 4.39 ppm) appeared in a higher magnetic field region than those of the fullerene reference $[Si_2]-C_{60}$ (δ_H 3.83, 4.51, and 4.72 ppm) and are attributed to the shielding effect of the porphyrin ring. The formation of folded conformers is also in agreement with the observation of the greatest shift for $ZnP-[Si_2]-C_{60}$, in which the ZnP moiety can approach the C_{60} moiety most easily ("sila-Hirayama rule").[13] Folded conformers are supposed to be in fast equilibrium with extended conformers (an example for $n = 5$ in Figure 2B), and averaged signals could not be separated even at low temperatures. Distribution of the conformers will be discussed on the basis of fluorescence decay dynamics.

2.2. Steady-State Absorption Spectra. The steady-state absorption spectra also afforded the information on the structural aspects of the $ZnP-[Si_n]-C_{60}$ molecules in the ground state. Figure 3 shows the spectra of $ZnP-[Si_1]-C_{60}$, $ZnP-[Si_5]-$

Bridge-Length Dependence of ZnP−[Si$_n$]−C$_{60}$

J. Phys. Chem. A, Vol. 111, No. 16, 2007 **2975**

TABLE 1: Steady-State Absorption and Fluorescence Spectral Data of ZnP−[Si$_n$]−C$_{60}$ in PhCN

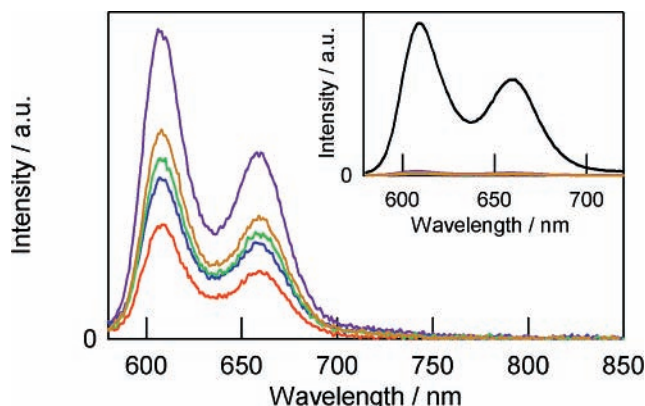|	absorption	fluorescence	
	γ^{ABS}_{max}/nm (ϵ/M^{-1} cm^{-1})	γ^{FL}_{max}/nm	relΦ_F
ZnP−[Si$_1$]−C$_{60}$	431.5 (5.86 × 10^5)	606, 658	0.026
	562.5 (2.06 × 10^4)		
	603.0 (1.18 × 10^4)		
ZnP−[Si$_2$]−C$_{60}$	437.5 (3.10 × 10^5)	609, 658	0.0097
	563.5 (1.69 × 10^4)		
	604.0 (1.05 × 10^4)		
ZnP−[Si$_3$]−C$_{60}$	437.5 (3.14 × 10^5)	607, 657	0.014
	563.5 (1.66 × 10^4)		
	603.5 (1.05 × 10^4)		
ZnP−[Si$_4$]−C$_{60}$	437.5 (3.12 × 10^5)	607, 657	0.015
	563.5 (1.64 × 10^4)		
	604.0 (1.07 × 10^4)		
ZnP−[Si$_5$]−C$_{60}$	437.5 (3.30 × 10^5)	608, 659	0.017
	563.0 (1.66 × 10^4)		
	603.5 (1.04 × 10^4)		
ZnP−[Si$_2$]	431.0 (5.72 × 10^5)	609, 661	
	561.0 (2.02 × 10^4)		
	602.5 (1.15 × 10^4)		

C$_{60}$, and the reference compound ZnP−[Si$_2$] in benzonitrile (PhCN) at room temperature. The absorption spectra of ZnP− [Si$_n$]−C$_{60}$ (n = 2−4) are similar to that of n = 5, as summarized in Table 1, in which the absorption maxima and molar extinction coefficients are listed.

The spectrum of ZnP−[Si$_1$]−C$_{60}$ is almost identical to that of ZnP−[Si$_2$], suggesting that there is no significant interaction between the ZnP and C$_{60}$ moieties in the ground state. In contrast, the spectrum of ZnP−[Si$_5$]−C$_{60}$ shows the characteristics of molecules that have an interaction between the ZnP and C$_{60}$ moieties; that is, the absorption coefficient (ϵ) at the Soret-band peak of ZnP−[Si$_5$]−C$_{60}$ is about half of that of ZnP− [Si$_2$], with a 6.5 nm red shift of the peak wavelength. In addition, the Q-band peaks of ZnP−[Si$_5$]−C$_{60}$ broaden compared to that of ZnP−[Si$_2$], and a weak broad absorption band was observed in the NIR region, where no absorption exists in ZnP−[Si$_2$]. These results also support the existence of folded conformers for ZnP−[Si$_n$]−C$_{60}$ with $n \geq 2$.[5k−m,8] In the case of ZnP−[Si$_1$]− C$_{60}$, the inflexible short linkage separates the ZnP and C$_{60}$ moieties from each other, and thus the perturbations due to the ZnP−C$_{60}$ interaction are smaller than other ZnP−[Si$_n$]−C$_{60}$ in the ground state.

2.3. Steady-State Fluorescence Spectra. Figure 4 shows the steady-state fluorescence spectra of ZnP−[Si$_n$]−C$_{60}$ and ZnP− [Si$_2$] excited at 560 nm where the concentrations of all PhCN solutions were adjusted to give the same absorbance. The spectral shapes of ZnP−[Si$_n$]−C$_{60}$ are almost the same as that of ZnP−[Si$_2$], which indicates that the emission occurs from the locally excited state of the ZnP moiety as a mirror image of the Q-absorption band. The energy level of the singlet-excited (S$_1$) state of the ZnP moiety was evaluated to be 2.03 eV on the basis of the intersection (605−607 nm) of the normalized absorption and fluorescence spectra.

The relative fluorescence quantum yields (relΦ_F) of ZnP− [Si$_n$]−C$_{60}$ to ZnP−[Si$_2$] reference are summarized in Table 1.[14,15] The relΦ_F values were 0.0097−0.026, indicating the existence of quenching paths of the ZnP fluorescence in the presence of the C$_{60}$ moiety. The cause of these results will be revealed in a later section through comparison with fluorescence lifetime.

2.4. Electrochemistry. The values of the first oxidation potentials (E_{ox}) of ZnP moiety and the reduction potentials (E_{red}) of C$_{60}$ moiety together with the differences between these potentials (ΔE) for ZnP−[Si$_n$]−C$_{60}$ in PhCN are summarized in Table 2 together with the E_{ox} value of ZnP−[Si$_2$] and the

Figure 4. Steady-state fluorescence spectra of ZnP−[Si$_n$]−C$_{60}$ excited by 560 nm light in PhCN; n = 1 (purple), 2 (orange), 3 (blue), 4 (green), and 5 (brown). Inset: Spectra of the ZnP−[Si$_n$]−C$_{60}$ with ZnP−[Si$_2$] (black).

TABLE 2: First Oxidation Potential (E_{ox}), First Reduction Potential (E_{red}), and Difference between E_{ox} and E_{red} (ΔE) of ZnP−[Si$_n$]−C$_{60}$, ZnP−[Si$_2$], and [Si$_2$]−C$_{60}$ in PhCN (vs Fc/Fc$^+$)

	E_{ox}/V	E_{red}/V	ΔE/V
ZnP−[Si$_1$]−C$_{60}$	0.30	−1.04	1.34
ZnP−[Si$_2$]−C$_{60}$	0.27	−1.08	1.35
ZnP−[Si$_3$]−C$_{60}$	0.27	−1.07	1.34
ZnP−[Si$_4$]−C$_{60}$	0.27	−1.10	1.37
ZnP−[Si$_5$]−C$_{60}$	0.27	−1.10	1.37
ZnP−[Si$_2$]	0.30		
[Si$_2$]−C$_{60}$		−1.04	

E_{red} value of [Si$_2$]−C$_{60}$. The E_{ox} and E_{red} values of ZnP−[Si$_1$]− C$_{60}$ are the same as E_{ox} value of ZnP−[Si$_2$] and the E_{red} value of [Si$_2$]−C$_{60}$, respectively. On the other hand, these values of ZnP−[Si$_n$]−C$_{60}$ with $n \geq 2$ are slightly negative (0.03−0.06 V) compared to those of ZnP−[Si$_1$]−C$_{60}$. These results suggest that the ground-state interaction only slightly affects the oxidation and reduction potentials, as observed even in the reported system in which the ZnP and C$_{60}$ moieties have significant electronic interaction with each other.[7e] The energy levels of the charge-separated states of the extended conformers can be represented by ΔE, since the electrostatic interaction between the radical-cation and radical-anion moieties would be small in the extended conformers. It is also expected that the energy levels of the charge-separated states of the folded conformers are lower than those of the extended conformers because of the larger electrostatic interaction. In most cases, the charge-separated states should be placed energetically lower than those of the S$_1$ states of the ZnP and C$_{60}$ moieties (2.03 and 1.73 eV,[16] respectively). Therefore, charge-separation (CS) processes can occur from the S$_1$ states of the ZnP and C$_{60}$ moieties of ZnP−[Si$_n$]−C$_{60}$.

2.5. Fluorescence Time-Profile Measurements. *2.5.1. ZnP-Fluorescence.* Fluorescence time-profiles of the ZnP moieties of ZnP−[Si$_n$]−C$_{60}$ and ZnP−[Si$_2$] in PhCN are shown in Figure 5. In the first instance, the decay curves of ZnP−[Si$_n$]−C$_{60}$ with $n \geq 2$ were fitted with a triexponential function to give the fluorescence lifetimes, while the decay curve of ZnP−[Si$_1$]− C$_{60}$ was fitted satisfactorily with a biexponential function to give two lifetimes. The slowest components were almost identical to the fluorescence lifetime of ZnP−[Si$_2$], suggesting that the origin of these components is attributable to the ZnP parts of the decomposed ZnP−[Si$_n$]−C$_{60}$ because of the repeated irradiations of the pulsed femtosecond laser light for the fluorescence time-profile measurements. For better understanding, therefore, all the fluorescence time-profiles were fitted
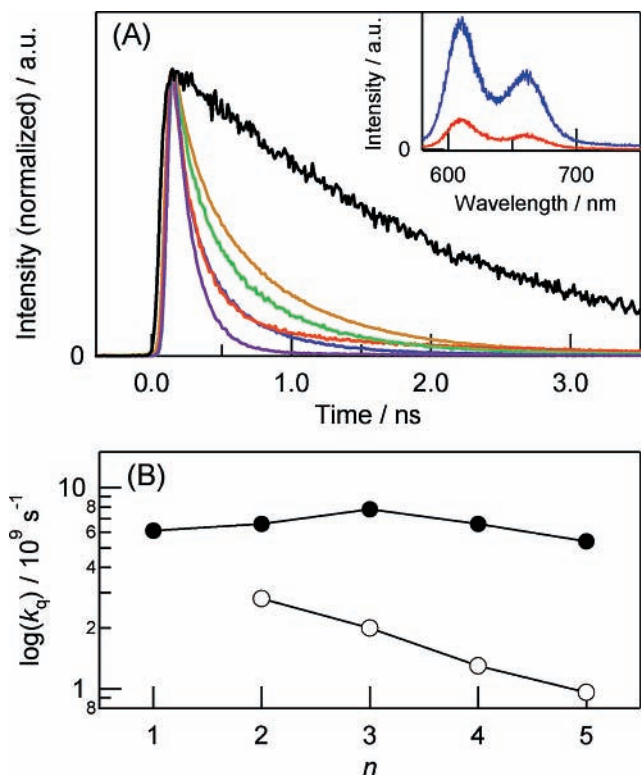
Figure 5. (A) Fluorescence time-profiles of ZnP−[Si$_n$]−C$_{60}$ with n = 1 (purple), 2 (orange), 3 (blue), 4 (green), and 5 (brown) and ZnP−[Si$_2$] (black) in PhCN. Intensities were normalized at the maximum intensities. Inset: Time-resolved fluorescence spectra of ZnP−[Si$_5$]−C$_{60}$ in PhCN at 0.1 ns (blue) and 1.0 ns (red). (B) Plots of k_{q1} (filled circle) and k_{q2} (open circle) against number of bridging dimethylsilylene units (n).

again, under the restriction that τ_{F3} was fixed to the lifetime of ZnP−[Si$_2$] (1.88 ns). The results are listed in Table 3, in which, for $n \geq 2$, the short, middle, and long lifetimes are denoted as τ_{F1}, τ_{F2}, and τ_{F3}, respectively, and for $n = 1$, the short and long lifetimes are denoted as τ_{F1} and τ_{F3}, respectively. The fluorescence-quenching rate constants (k_{q1}, k_{q2})[17] calculated from the τ_{F1} and τ_{F2} values are also listed in Table 3. As displayed in Figure 5B, the k_{q2} values tend to decrease with increasing of the silicon-chain length ($n \geq 2$), while the k_{q1} values are invariant with the bridge length. These bridge-length dependences will be interpreted in a later section.

To evaluate the fluorescence quantum yield from the fluorescence lifetimes, relative fluorescence lifetimes (relτ_F) were calculated using the following equation:

$$\mathrm{rel}\tau_F = \tau_{F,\mathrm{ave}}^{\mathrm{dyad}}/\tau_F^{\mathrm{ref}} \qquad (1)$$

where $\tau_{F,\mathrm{ave}}^{\mathrm{dyad}}$ is the averaged fluorescence lifetime of the τ_{F1}

and τ_{F2} values without considering the slowest component (τ_{F3}), and τ_F^{ref} is the fluorescence lifetime of ZnP−[Si$_2$]. The values of relτ_F are summarized in Table 3. Since fluorescence quantum yield is known to be proportional to fluorescence lifetime in the presence of quenching source,[18] relτ_F values are expected to be the same as relΦ_F values. However, the relτ_F values are almost 10−20 times larger than the relΦ_F values. This difference can be rationalized by assuming that the majority of the molecules are nonemissive. As the origin of this phenomenon, we postulate the followings: (1) the fluorescence is emitted from the extended conformers, and the folded conformers are nonemissive. The latter point can be supported by the well-known fact that the species which have interaction between the ZnP and C$_{60}$ moieties immediately form very short lifetime excited-state CT complexes upon photoexcitation.[5k−m,10] However, the shortest observed lifetimes (τ_{F1} = 120−170 ps) are too long to assign to such excited-state CT complexes, which supports the former point. In addition, the steady-state fluorescence spectra did not show CT emission. (2) The rate of the folded−extended conformational change is much smaller than that of the fluorescence quenching and, therefore, what we observed in the fluorescence lifetime measurements are the processes via the excited states of extended conformers. The slow conformational change is supported by the fluorescence time-profile measurements at various temperatures (see Figure S1 and Table S1 in Supporting Information), in which the fluorescence lifetimes of ZnP−[Si$_1$]−C$_{60}$ and ZnP−[Si$_5$]−C$_{60}$ were not affected by the deceleration of the conformational change with lowering the temperatures.

2.5.2. C$_{60}$-Fluorescence. As for the C$_{60}$ moiety, distinguishable emission band from the C$_{60}$ moiety could not be observed even after the ZnP fluorescence completely vanished in the time-resolved fluorescence spectra as shown in the inset of Figure 5A. Although photoirradiation could form the S$_1$ state of C$_{60}$, followed by quenching via ET, the fluorescence intensity of the C$_{60}$ moiety was too low to detect with our measurement system because of the overlap with the strong ZnP emission band.

2.6. Time-Resolved Transient Absorption Measurements.
2.6.1. Time-Resolved Transient Absorption Spectra. The time-resolved transient absorption spectra of ZnP−[Si$_5$]−C$_{60}$ excited by 532 nm laser light in Ar-saturated PhCN solution are shown in Figure 6, and almost the same spectra were obtained for other ZnP−[Si$_n$]−C$_{60}$ including $n = 1$. The depression around 600 nm at 0.1 μs is due to the lack of the Q-band absorption in the ground state. The transient absorption bands appearing around 1000 nm and at a shorter wavelength than 660 nm are attributed to the radical anion of the C$_{60}$ moiety and the radical cation of the ZnP moiety, respectively.[19,20] These bands decayed in the order of sub-microseconds (see Table 4). Because the absorption bands arose immediately after laser pulse irradiation, the

TABLE 3: Fluorescence Lifetime (τ_F), Correlation Coefficient (R), Rate Constant of Fluorescence Quenching (k_q), Quantum Yield of Charge Separation of Extended Conformers (Φ_{CS}), and Relative Fluorescence Lifetime (relτ_F) of ZnP−[Si$_n$]−C$_{60}$ and ZnP−[Si$_2$] in PhCN

	τ_F/ns (fraction/%)				$k_q/10^9$ s^{-1}			
	τ_{F1}	τ_{F2}	τ_{F3}[b]	R	k_{q1}	k_{q2}	Φ_{CS}[c]	relτ_F
ZnP−[Si$_1$]−C$_{60}$[a]	0.15 (99)		1.88 (1)	0.9990	6.1		0.92	0.08
ZnP−[Si$_2$]−C$_{60}$	0.14 (62)	0.30 (28)	1.88 (10)	0.9999	6.6	2.8	0.90	0.10
ZnP−[Si$_3$]−C$_{60}$	0.12 (49)	0.39 (49)	1.88 (2)	>0.9999	7.8	2.0	0.86	0.14
ZnP−[Si$_4$]−C$_{60}$	0.14 (37)	0.54 (59)	1.88 (3)	0.9999	6.6	1.3	0.79	0.21
ZnP−[Si$_5$]−C$_{60}$	0.17 (33)	0.67 (62)	1.88 (5)	0.9999	5.4	0.96	0.74	0.26
ZnP−[Si$_2$]			1.88 (100)	0.9975				

[a] Fitted with biexponential function. [b] Fixed to 1.88 ns for ZnP−[Si$_n$]−C$_{60}$. [c] $\Phi_{CS} = (1/\tau_{F,\mathrm{ave}}^{\mathrm{dyad}} - 1/\tau_F^{\mathrm{ref}})/(1/\tau_{F,\mathrm{ave}}^{\mathrm{dyad}})$.

Figure 6. Time-resolved transient absorption spectra of ZnP$-$[Si$_5$]$-$C$_{60}$ in PhCN (0.15 mM) at 0.1 μs (white circle) and 1.0 μs (black circle) after photoexcitation by 532 nm laser light. Inset: Absorption time-profiles at 640 nm (dotted line) and 1000 nm (solid line).

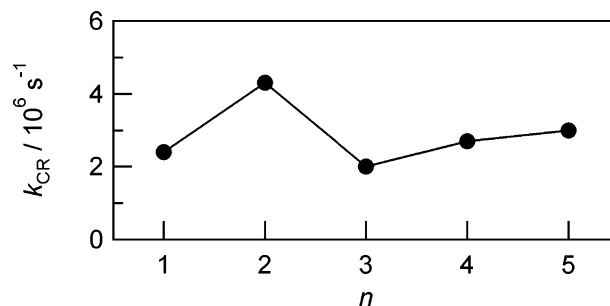**Figure 7.** Plots of rate constant of charge recombination (k_{CR}) against number of bridging dimethylsilylene units (n).

TABLE 4: Rate Constant of Charge Recombination (k_{CR}) and Lifetime of Radical-Ion Pair (τ_{RIP}) of ZnP$-$[Si$_n$]$-$C$_{60}$ in PhCN

	$k_{CR}/10^6$ s^{-1}	τ_{RIP}/μs
ZnP$-$[Si$_1$]$-$C$_{60}$	2.4	0.41
ZnP$-$[Si$_2$]$-$C$_{60}$	4.3	0.23
ZnP$-$[Si$_3$]$-$C$_{60}$	2.0	0.50
ZnP$-$[Si$_4$]$-$C$_{60}$	2.7	0.37
ZnP$-$[Si$_5$]$-$C$_{60}$	3.0	0.33

generation of the radical-ion pair of ZnP$-$[Si$_5$]$-$C$_{60}$ is an intramolecular process.

2.6.2. Lifetimes of Radical-Ion Pairs. The decays of both the radical-cation and anion absorption bands were fitted well by monoexponential function, affording the rate constants of charge recombination (k_{CR}) as summarized in Table 4, in which the lifetimes of radical-ion pairs (τ_{RIP}) are also listed. It is reasonable to assume that the τ_{RIP} values with sub-microsecond lifetimes correspond to the radical-ion pairs of the extended conformers, but not to the folded conformers, on the basis of the following reasons: (1) the observed lifetimes are within the range of reported values of the radical-ion pairs in the ZnP$-$C$_{60}$ molecules that have little interaction between the ZnP and C$_{60}$ moieties[5n,7f] but much longer than the typical lifetime of those of the folded conformers (of the order of picoseconds)[5l] and (2) the quantum yield of the CS (Φ_{CS}), which was evaluated by the nanosecond time-resolved transient absorption measurements, of ZnP$-$[Si$_1$]$-$C$_{60}$ with less ZnP$-$C$_{60}$ electronic interaction is higher than that of ZnP$-$[Si$_5$]$-$C$_{60}$ (see Figure S2 and Table S2 in Supporting Information).

The k_{CR} values do not vary linearly with the number of silicon atoms as plotted in Figure 7. Considering that the rates of through-bond ET via a superexchange mechanism would vary regularly with the bridge length, through-bond ET from extended conformers is not a major process. It can be postulated that one of the major processes causing the charge recombination is the extended-to-folded conformational changes, followed by fast intramolecular through-space charge recombination.

3. Discussion

3.1. Mechanism of Charge Separation. The most probable quenching path responsible for the shortening of fluorescence lifetimes of the extended conformers is the ET process from the S$_1$ state of the ZnP moiety to the C$_{60}$ moiety, similar to other covalently linked ZnP$-$C$_{60}$ systems.[5o] The observed two-

component decay for ZnP$-$[Si$_n$]$-$C$_{60}$ with $n \geq 2$ can be attributed to the existence of two conformers within the extended conformers. On the basis of the bridge-length dependences of the quenching rate constants (k_{q1} and k_{q2}) and of the fractions of these two rate constants, we propose the following assignments for k_{q1} and k_{q2} of ZnP$-$[Si$_n$]$-$C$_{60}$ with $n \geq 2$: (1) the faster fluorescence quenching process (k_{q1}) is through-space ET in families of short-extended conformers in which the oligosilane chain is partly extended resulting in relatively short ZnP$-$C$_{60}$ distance, and the spatial distances between the ZnP and C$_{60}$ moieties of the families of short-extended conformers are almost the same for all ZnP$-$[Si$_n$]$-$C$_{60}$ with $n \geq 2$ and (2) the slower one (k_{q2}) is through-bond ET in families of long-extended conformers in which the oligosilane chain is extended enough to minimize the rate of through-space ET. The families of short-extended conformers should not be categorized as folded conformers.[21]

Assignment 1 is based on the observation that k_{q1} barely depends on the length of oligosilanes as shown in Figure 5B. It is well-known that the through-space process is possible only for short-range ET,[51] while through-bond ET governs CS process for molecules with longer donor$-$acceptor distance. Assignment 2 is based on the result that log k_{q2} linearly depends on the number of the silicon atoms, suggesting the occurrence of through-bond ET. If the ZnP$-$C$_{60}$ distance is small, through-space ET would be the dominant process. Thus, k_{q2} should be due to the CS of the families of long-extended conformers. Moreover, the bridge-length dependence of the fraction of the fluorescence lifetime components, that is, as n number increases, the fraction of k_{q1} decreases, and that of k_{q2} increases as shown in Table 3, supports these assignments. That is, the proportion of the families of long-extended conformers becomes large as the Si number increases because of the larger mobility of the longer oligosilane bridge.

As for $n = 1$, the families of short- and long-extended conformers should also be considered to understand the fluorescence quenching despite the one-component fluorescence decay (k_{q1}). This assumption is based on the result that extrapolation of the k_{q2} plot to $n = 1$ meets the k_{q1} value of ZnP$-$[Si$_1$]$-$C$_{60}$ as shown in Figure 5B. This result indicates that the rate of the through-bond ET in the families of long-extended conformers is almost the same as that of the through-space ET in the families of short-extended conformers because of short Si$_1$ bridge (see Figure 8).

3.2. Rate Constant of Charge Separation. The rate constants of the through-bond ET of ZnP$-$[Si$_n$]$-$C$_{60}$, which correspond to the k_{q2} values (($0.96-2.8) \times 10^9$ s^{-1}), are smaller than those reported for ZnP$-$C$_{60}$ dyads linked by π-conjugated carbon-based bridges, such as diphenylamide (9.5×10^9 s^{-1})[5j$-$o] and diphenylacetylene (3.0×10^{10} s^{-1}).[7f] These differences can be explained by the comparison of lowest unoccupied molecular

(A)

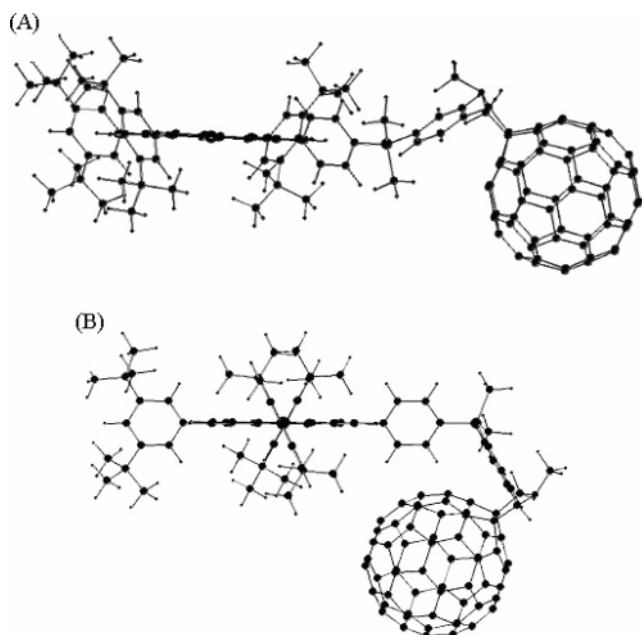(B)

Figure 8. Representative structures of families of long-extended (A) and short-extended (B) conformers of ZnP$-$[Si$_1$]$-$C$_{60}$ optimized with molecular mechanics method using UFF force field.

orbital (LUMO) energy gaps between ZnP and bridges, because the ET in these systems is supposed to occur via superexchange mechanism, in which the ET rate should decrease with increasing the energy gap between the initial state and the virtual charge-separated state resulting from the ET from donor to bridge. The calculated LUMO levels of 1,2-diphenyl-1,1,2,2-tetramethyldisilane, *N*-phenylbenzamide, diphenylacetylene, and ZnP are 2.88, 2.25, 1.98, and 0.35 eV, respectively (HF/6-311G*//B3LYP/6-31G*). Such a large LUMO energy gap between ZnP and oligosilane relative to π-conjugated carbon-based bridges would be one of the origins of such slow ET rates of the present oligosilane-bridged ZnP$-$C$_{60}$ molecules.

3.3. Attenuation Factor of Oligosilane. Because the families of short-extended conformers of ZnP$-$[Si$_n$]$-$C$_{60}$ have almost the same ZnP$-$C$_{60}$ distance, it does not make sense to evaluate the β value for through-space ET from the slope of plot of log k_{q1} versus the number of the dimethylsilylene units of the oligosilane bridges (*n*) as shown in Figure 5B. On the other hand, the β value of the through-bond ET can be estimated from the slope of the plot of log k_{q2}. The k_{q2} values of $n \geq 2$ were used for the estimation because through-bond ET rates are distinguishable from through-space ET rates. Applying a Si$-$Si length of 2.34 Å,[22] the β value is estimated to be 0.16 Å^{-1}. The small β value, which is the same order as those of carbon π-conjugated bridges,[23] suggests that the oligosilane is an excellent molecular wire.

4. Conclusion

A series of oligosilane-bridged zinc porphyrin$-$fullerene molecules ZnP$-$[Si$_n$]$-$C$_{60}$ with various bridge lengths (*n* = 1$-$5) was newly synthesized, and their photophysical properties were investigated using conventional and time-resolved spectroscopic methods. The ^{1}H NMR and steady-state absorption measurements indicate that ZnP$-$[Si$_n$]$-$C$_{60}$ involve extended and folded conformers. The results of the steady-state fluorescence and fluorescence time-profile measurements suggest that the photoexcitation of the folded conformers forms nonemissive short-lived excited CT states, while the fluorescence quenching paths of the S$_1$ states of ZnP moieties of the extended conformers

are attributed to the competitive through-space and trough-bond ET. The transient absorption measurements unambiguously demonstrate the formation of the radical-ion pair with a lifetime of sub-microseconds. The through-bond ET of the present ZnP$-$[Si$_n$]$-$C$_{60}$ molecules is slower than those of other Zn$-$C$_{60}$ dyads because of the large energy gap between LUMO orbitals of ZnP and oligosilane as confirmed by MO calculations. The β value of the ET of the σ-conjugated oligosilane bridge was evaluated for the first time to be 0.16 Å^{-1} on the basis of the bridge-length dependent component of the CS process, which is the same level as those of the other bridges comprising π-conjugated carbon-based systems. These results indicate that the oligosilane σ-conjugation system works well as a good molecular wire for a long-range CS and is promising material applicable to photovoltaic devices and so forth.

5. Experimental Section

Apparatus. Steady-state absorption spectra in the visible to near-IR regions were measured on a spectrophotometer (Jasco, V570 DS). Steady-state fluorescence spectra were measured on a spectrofluorophotometer (Shimazu, RF-5300 PC). Electrochemical measurements were carried out with Osteryoung square wave voltammetry method using a potentiostat (BAS, CV-50W) in a conventional three-electrode cell equipped with Pt working electrode, counter electrode, and Ag/AgCl reference electrode in the presence of tetrabutylammonium perchlorate as an electrolyte at room temperature. The solutions for the electrochemical measurements were deaerated by bubbling Ar gas for 20 min.

The fluorescence time-profiles were measured by a single-photon-counting method using a streakscope (Hamamatsu Photonics, C4334-01) equipped with a polychrometor and a second-harmonic generation (400 nm) of a Ti:sapphire laser (Spectra-Physics, Tsunami 3950-L2S, 150 fs fwhm) as an excitation source.

Nanosecond laser flash photolysis experiments were carried out using the 532 nm light from second-harmonic generation of a Nd:YAG laser (Spectra-Physics, Quanta-Ray, GCR-130, 6 ns fwhm) as excitation source. For the transient absorption spectra in the near-IR region (600$-$1200 nm), monitoring light from a pulsed Xe lamp was detected with a Ge-APD detector. For spectra in the visible region (400$-$600 nm), a Si$-$PIN photodiode was used as a detector. All the sample solutions in a quartz cell (1 cm $\times$ 1 cm) were deaerated by bubbling Ar gas through the solution for 15 min.

Supporting Information Available: Synthesis of ZnP$-$[Si$_n$]$-$C$_{60}$; the temperature dependence of the fluorescence lifetime and the time-resolved transient absorption spectra of ZnP$-$[Si$_1$]$-$C$_{60}$ and ZnP$-$[Si$_5$]$-$C$_{60}$ at 0.1 ns are included. This material is available free of charge via the Internet at http://pubs.acs.org.

References and Notes

(1) In *The Photosynthetic Reaction Center*; Deisenhofer, J., Norris, J. R., Eds.; Academic Press: New York, 1993.

(2) Kavarnos, G. *Top. Curr. Chem.* **1990**, *156*, 21.

(3) (a) McConnell, H. M. *J. Chem. Phys.* **1961**, *35*, 508. (b) Jotner, J.; Bixon, M. In *Protein Structure: Molecular and Electronic Reactivity*; Austin, R., Buhks, E., Chance, B., DeVault, D., Dutton, P. L., Frauenfelder, H., Goldanskii, V. I., Eds.; Springer: New York, 1985; p 277. (c) Weiss, E. A.; Tauber, M. J.; Kelley, R. F.; Ahrens, M. J.; Ratner, M. A.; Wasielewski, M. R. *J. Am. Chem. Soc.* **2005**, *127*, 11842. (d) Giacalone, F.; Segura, J. L.; Martín, N.; Ramey, J.; Guldi, D. M. *Chem.$-$Eur. J.* **2005**, *11*, 4819.

(4) (a) Pasman, P.; Koper, N. W.; Verhoeven, J. W. *Recl. Trav. Chim. Pays$-$Bas.* **1982**, *101*, 363. (b) Hush, N. S.; Paddon-Row, M. N.; Cotsaris, E.; Oevering, H.; Verhoeven, J. W.; Heppener, M. *Chem. Phys. Lett.* **1985**, *117*, 8. (c) Closs, G. L.; Piotrowiak, P.; MacInnis, J. M.; Fleming, G. R. *J. Am. Chem. Soc.* **1988**, *110*, 2652. (d) Paddon-Row, M. N.; Oliver, A. M.; Warman, J. M.; Smit, K. J.; De Haas, M. P.; Oevering, H.; Verhoeven, J. W. *J. Phys. Chem.* **1988**, *92*, 6958.

(5) (a) Yang, N. C.; Neoh, S. B.; Naito, T.; Ng, L.-K.; Chernoff, D. A.; McDonald, D. B. *J. Am. Chem. Soc.* **1980**, *102*, 2806. (b) Crawford, M. K.; Wang, Y.; Eisenthal, K. B. *Chem. Phys. Lett.* **1981**, *79*, 529. (c) Siemiarczuk, A.; McIntosh, A. R.; Ho, T.-H.; Stillman, M. J.; Roach, K. J.; Weedon, A. C.; Bolton, J. R.; Connoly, J. S. *J. Am. Chem. Soc.* **1981**, *105*, 7224. (d) Luo, X. J.; Beddard, G. S.; Porter, G.; Davidson, R. S.; Whelan, T. D. *J. Chem. Soc., Faraday Trans. 1* **1982**, *78*, 3467. (e) Wang, Y.; Crawford, M. C.; Eisenthal, K. B. *J. Am. Chem. Soc.* **1982**, *104*, 5874. (f) Grabowski, Z.; Dobkowski, J. *J. Pure Appl. Chem.* **1983**, 295. (g) McIntosh, A. R.; Siemiarczuk, A.; Bolton, J. R.; Stillman, M. J.; Ho, T.-H.; Weedon, A. C. *J. Am. Chem. Soc.* **1983**, *105*, 7215. (h) Mataga, N. *Pure Appl. Chem.* **1984**, *56*, 1255. (i) Batteas, J. D.; Harriman, A.; Kanda, Y.; Mataga, N.; Nowak, A. K. *J. Am. Chem. Soc.* **1990**, *112*, 126. (j) Imahori, H.; Sakata, Y. *Adv. Mater.* **1997**, *9*, 537. (k) Imahori, H.; Sakata, Y. *Eur. J. Org. Chem.* **1999**, *10*, 2445. (k) Kesti, T. J.; Tkachenko, N. V.; Vehmanen, V.; Yamada, H.; Imahori, H.; Fukuzumi, S.; Lemmetyinen, H. *J. Am. Chem. Soc.* **2002**, *124*, 8067. (l) Tkachenko, N. V.; Lemmetyinen, H.; Sonoda, J.; Ohkubo, K.; Sato, T.; Imahori, H.; Fukuzumi, S. *J. Phys. Chem. A* **2003**, *107*, 8834. (m) Imahori, H. *Org. Biomol. Chem.* **2004**, *2*, 1425. (n) Imahori, H.; Sekiguchi, Y.; Kashiwagi, Y.; Sato, T.; Araki, Y.; Ito, O.; Yamada, H.; Fukuzumi, S. *Chem.$-$Eur. J.* **2004**, *10*, 3184. (o) Imahori, H.; Tamaki, K.; Guldi, D. M.; Luo, C.; Fujitsuka, M.; Ito, O.; Sakata, Y.; Fukuzumi, S. *J. Am. Chem. Soc.* **2001**, *123*, 2607.

(6) (a) Wasielewski, M. R. *Chem. Rev.* **1992**, *92*, 435. (b) Gust, D.; Moore, T. A.; Moore, A. L. *Acc. Chem. Res.* **1993**, *26*, 198. (c) Liddel, P.; Macpherson, A. N.; Sumida, J.; Demanche, L.; Moore, A. L.; Moore, T. A. Gust, D. *Photochem. Photobiol.* **1994**, *59S*, 36S. (d) Harriman, A.; Sauvage, J. P. *Chem. Soc. Rev.* **1996**, *25*, 41. (e) Osuka, A.; Mataga, N.; Okada, T. *Pure Appl. Chem.* **1997**, *69*, 797. (f) Imahori, H.; Tamaki, K.; Yamada, H.; Yamada, K.; Sakata, Y.; Nishimura, Y.; Yamazaki, I.; Fujitsuka, M.; Ito, O. *Carbon* **2000**, *38*, 1599. (g) El-Khouly, M. E.; Ito, O.; Smith, P. M.; D'Souza, F. *J. Photochem. Photobiol. C* **2004**, *5*, 79. (h) Harriman, A. *Angew. Chem., Int. Ed.* **2004**, *43*, 4985. (i) Imahori, H. *Org. Biomol. Chem.* **2004**, *2*, 1425.

(7) (a) Imahori, H.; Cardoso, S.; Tatman, D.; Lin, S.; Noss, L.; Seely, G. R.; Sereno, L.; de Silber, J. C.; Moore, T. A.; Moore, A. L.; Gust, D. *Photochem. Photobiol.* **1995**, *62*, 1009. (b) Kuciauskas, D.; Lin, S.; Seely, G. R.; Moore, A. L.; Moore, T. A.; Gust, D.; Drovetskaya, T.; Reed, C.; Boyd, P. D. W. *J. Phys. Chem.* **1996**, *100*, 15926. (c) Liddell, P. A.; Kuciauskas, D.; Sumida, J. P.; Nash, B.; Nguyen, D.; Moore, A. L.; Moore, T. A.; Gust, D. *J. Am. Chem. Soc.* **1997**, *119*, 1400. (d) Yamada, K.; Imahori, H.; Nishimura, Y.; Yamazaki, I.; Sakata, Y. *Chem. Lett.* **1999**, *28*, 895. (e) Armaroli, N.; Marconi, G.; Echegoyen, L.; Bourgeois, J.-P.; Diederich, F. *Chem.$-$Eur. J.* **2000**, *6*, 1629. (f) Imahori, H.; Yamada, H.; Guldi, D. M.; Endo, Y.; Shimomura, A.; Kundu, S.; Yamada, K.; Okada, T.; Sakata, Y.; Fukuzumi, S. *Angew. Chem., Int. Ed.* **2002**, *41*, 2344.

(8) (a) Tsuji, H.; Sasaki, M.; Shibano, Y.; Toganoh, M.; Kataoka, T.; Araki, Y.; Tamao, K.; Ito, O. *Bull. Chem. Soc. Jpn.* **2006**, *79*, 1338. (b) Shibano, Y.; Sasaki, M.; Tsuji, H.; Araki, Y.; Ito, O.; Tamao, K. *J. Organomet. Chem.* **2007**, *692*, 356. (c) Sasaki, M.; Shibano, Y.; Tsuji, H.; Araki, Y.; Tamao, K.; Ito, O. *Electrochem. Soc. Trans.* **2007**, *2*, 29.

(9) (a) Kumada, M.; Tamao, K. *Adv. Organomet. Chem.* **1968**, *19*, 6. (b) Kira, M.; Miyazawa, T. In *The Chemistry of Organosilicon Compounds*; Rappoport, Z., Apeloig, Y., Eds.; Vol. 2; Wiley: Chichester, U.K.,1998; p 1311. (c) Tsuji, H.; Michl, J.; Tamao, K. *J. Organomet. Chem.* **2003**, *685*, 9.

(10) (a) Kepler, R. G.; Zeigler, J. M.; Harrah, L. A.; Kurtz, S. R. *Phys. Rev. B* **1987**, *35*, 2818. (b) Pope, M.; Swenberg, C. *Electronic Processes in Organic Crystals and Polymers,* 2nd ed.; Oxford University Press: New York, 1999; Chapter 11. (c) Abkowitz, M.; Bässler, H.; Stolka, M.; *Philos. Mag. B* **1991**, *63*, 201. (d) Kepler, R. G.; Cahill, P. A. *Appl. Phys. Lett.* **1993**, *63*, 1552. (e) Watanabe, A.; Ito, O. *J. Phys. Chem.* **1994**, *98*, 7736.

(11) For example, Pasquarello, A.; Schlüter, M.; Haddon, R. C. *Science* **1992**, *257*, 1660.

(12) For example, Kruper, W. J.; Chamberlin, T. A.; Kochanny, M. *J. Org. Chem.* **1989**, *54*, 2753.

(13) (a) Karatsu, T.; Shibata, T.; Nishigaki, A.; Kitamura, A.; Hatanaka, Y.; Nishimura, Y.; Sato, S.; Yamazaki, I. *J. Phys. Chem. B* **2003**, *107*, 12184. (b) Karatsu, T.; Terasawa, M.; Yagai, S.; Kitamura, A.; Nakamura, T.; Nishimura, Y.; Yamazaki, I. *J. Organomet. Chem.* **2004**, *689*, 1029.

(14) The areas of fluorescence spectra were calculated in the range between 11765 and 17544 cm^{-1} corresponding to 570$-$850 nm.

(15) rel$\Phi_F = \Phi_F^{dyad}/\Phi_F^{ref}$, where Φ_F^{dyad} and Φ_F^{ref} are the fluorescence-quantum yields of ZnP$-$[Si$_n$]$-$C$_{60}$ and ZnP$-$[Si$_2$], respectively, corresponding to the areas of the fluorescence spectra.

(16) The evaluation of the energy level of the S$_1$ state of the C$_{60}$ moiety was based on the intersection of the normalized absorption and fluorescence spectra of [Si$_2$]$-$C$_{60}$ in PhCN.

(17) $k_q = 1/\tau_F^{dyad} - 1/\tau_F^{ref}$, where τ_F^{dyad} and τ_F^{ref} are the fluorescence lifetimes of ZnP$-$[Si$_n$]$-$C$_{60}$ and ZnP$-$[Si$_2$] (1.88 ns), respectively.

(18) In *Handbook of Photochemistry*; Montalti, M., Credi, A., Prodi, L., Gandolfi, M. T., Eds.; CRC Press: Boca Raton, FL, 2006.

(19) Fuhrhop, J.-H.; Manzrall, D. J. *J. Am. Chem. Soc.* **1969**, *91*, 4174.

(20) Guldi, D. M.; Hungerbühlar, H.; Janata, E.; Asmus, K.-D. *J. Phys. Chem.* **1993**, *97*, 11258.

(21) This is a matter of the definition; we defined folded conformers as the species that cause the CT band in the steady-state absorption spectra and produce ultrashort lifetime excited CT state upon photoexcitation.

(22) Emsley, J. In *The Elements,* 3rd ed.; Oxford University Press: New York, 1998.

(23) (a) Osuka, A.; Maruyama, K.; Mataga, N.; Asahi, T.; Yamazaki, I.; Tamai, N. *J. Am. Chem. Soc.* **1990**, *112*, 4958. (b) Helms, A.; Heiler, D.; McLendon, G. *J. Am. Chem. Soc.* **1992**, *114*, 6227. (c) Benniston, A. C.; Goulle, V.; Harriman, A.; Lehn, J.-M.; Marczinke, B. *J. Phys. Chem.* **1994**, *98*, 7798. (d) Osuka, A.; Tanabe, N.; Kawabata, S.; Yamazaki, I.; Nishimura, Y. *J. Org. Chem.* **1995**, *60*, 7177. (e) Grosshenny, V.; Harriman, A.; Ziessel, R. *Angew. Chem., Int. Ed. Engl.* **1995**, *34*, 1100. (f) Grosshenny, V.; Harriman, A.; Ziessel, R. *Angew. Chem., Int. Ed. Engl.* **1995**, *34*, 2705. (g) Barigelletti, F.; Flamigni, L.; Guardigli, M.; Juris, A.; Beley, M.; Chodorowski-Kimmens, S.; Collins, J.-P.; Sauvage, J.-P. *Inorg. Chem.* **1996**, *35*, 136. (h) Schlicke, B.; Belser, P.; De Cola, L.; Sabbioni, E.; Balzani, V. *J. Am. Chem. Soc.* **1999**, *121*, 4207.